



0017-9310(94)E0047-X

Heat and mass transfer boundary layers in radial creeping flow

GIOVANNI CAMERA-RODA, CRISTIANA BOI, ALDO SAAVEDRA† and
 GIULIO C. SARTI

Dipartimento di Ingegneria Chimica e di Processo, Università degli Studi di Bologna,
 Viale Risorgimento 2, I 40136 Bologna, Italy

(Received 29 July 1993 and in final form 10 November 1993)

Abstract—Heat and mass transfer in radial flow between two parallel disks are analysed. This kind of problem is sometimes encountered in chemical engineering and we faced this situation in membrane separation processes in which the fluid is fed into the center of the cell and flows towards zones at higher radii. In the examined case heat and/or mass are exchanged across one of the two surfaces which confine the flow region. An analysis of the transport phenomena of such a geometry is performed by resorting to two different mathematical models. As a result the concentration and/or temperature profiles, the transport coefficients and the influence of the relevant dimensionless groups are obtained. The capability of the models to predict the experimental behavior of the vacuum membrane distillation process is demonstrated.

INTRODUCTION

THE FLOW of a fluid between two parallel disks from the center of the disks to the higher radii region is sometimes encountered in chemical engineering problems. Referring to the geometry represented in Fig. 1, when the flow is in the creeping regime the velocity profile is parabolic in the transverse z -direction [1] and according to the equation:

$$v_r(r, z) = 6v_m(r) \frac{z}{b} \left(1 - \frac{z}{b}\right), \quad (1)$$

and it is varying along the radius r as $v_m(r)$ is given by:

$$v_m(r) = \frac{\dot{V}}{2\pi b} \frac{1}{r}, \quad (2)$$

where \dot{V} is the volumetric flow rate. However, the most interesting problems in such a geometry involve also heat and/or mass transfer phenomena for which few experimental results and deficient theoretical developments and analysis are available in the literature. In particular the lack of fundamental works on this topic is especially important since the influence of the relevant dimensionless groups on the behavior of the system may be significantly different from that pertaining to the flow in other well-exploited geometries as through a cylindrical tube or between parallel plates. As a matter of fact there are many cases where radial flow is encountered accompanied by heat and mass transfer, and examples can be found in injec-

tion molding, membrane processes, and reactor operation.

Of course the appraisal and prediction of the transfer coefficients are essential to the analysis of the problems and are of primary importance in the design of the apparatus. We faced this situation in different studies on membrane separation for which, in many cases, the separation performances were determined by the transport processes taking place not only within the membrane but also in the external fluid phase which in our experiments was moving radially through parallel disks.

Unfortunately, the investigation of the problem is limited in the literature and apparently a sufficiently detailed study is still needed. The case of an unconfined stream impinging on a flat plate has been dealt with in ref. [2]; but the geometry and the relevant boundary conditions are substantially different from those we are interested in, so that the results and the conclusions obtained in ref. [2] can be extended to the current problem only under very special operative conditions. Indeed we are interested in the case in which heat and/or mass are exchanged only across one of the two surfaces which confine the flow region.

The current geometry was investigated by Stevenson [3], but the boundary conditions are not exactly the same which hold for most of the cases of practical interest. Furthermore in ref. [3] the influence of the relevant dimensionless groups is not apparent and is not analysed and, moreover, the existence of the boundary layers is disregarded. In addition the model can be used in practice with difficulty as the analytical expressions for the local concentration (or temperature) values are in the form of infinite series which

† Present address: Instituto de Agroindustria, Universidad de la Frontera, Temuco, Chile.

NOMENCLATURE

b	clearance between the disks	Greek symbols	
c	molar concentration in the liquid phase	α	thermal diffusivity
\hat{c}_p	heat capacity	Γ	heat or mass diffusivity
D	cell diameter	γ_i	activity coefficient
\mathcal{D}	mass diffusivity	δ	boundary layer thickness
h	heat transfer coefficient in the liquid phase	η	dimensionless independent group
J	molar flux	λ_i	molar latent heat of vaporization
k_L	mass transfer coefficient in the liquid phase	ν	kinematic viscosity
k	thermal conductivity	ρ	density
K_m	pore permeability, see equation (15)	ϕ	temperature or mass fraction of the permeating component.
M	molecular weight		
Nu	Nusselt number	Subscripts and superscripts	
P	pressure	av	average value
Pr	Prandtl number	B	bulk
r	radial coordinate	i	i th component
Re	Reynolds number	I	interface
Sc	Schmidt number	L	liquid
Sh	Sherwood number	m	mean
T	temperature	P	permeate
v	velocity	r	r -direction
\dot{V}	volumetric flow rate	t	total
x	mole fraction in the liquid phase	V	vapor
z	axial coordinate	w	wall
y	mole fraction in the vapor phase.	z	z -direction
		0	inlet
		*	dimensionless group.

may converge with difficulty [4, 5] and, in any case, the eigenvalues, which appear in those expressions, are obtained by rather complex numerical methods.

The aim of the present work is twofold: (1) to study from a fundamental point of view the problem; and (2) to develop suitable models which could be easily applied to the description of systems of practical interest, as those encountered in membrane separations.

So mathematical models will be considered and solved to get: (a) the concentration and/or tem-

perature profiles and, at the same time, the corresponding boundary layer properties; (b) the local and average transport coefficients; and (c) the influence of the relevant dimensionless groups. The examined models will be two of different complexities and the corresponding results will be compared with each other, in order to obtain information on the limits of validity of the simpler model. The comparison will be extended also to experimental data to demonstrate the usefulness of the fundamental study and the appli-

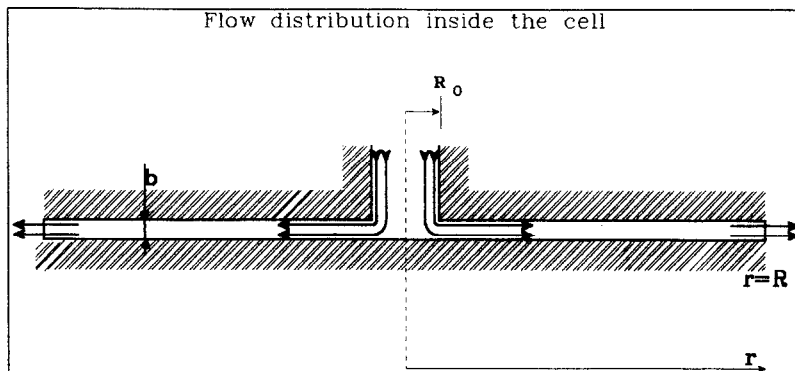


FIG. 1. Flow distribution inside the cell.

cability of the models to practical problems when heat and mass are transferred between the fluid phase and the surface of the disks. This situation holds in the examined membrane process.

Some considerations about the two models are now in order. In both of them the flow field is assumed to be independent of the temperature and concentration distribution. This is a likely hypothesis as long as the temperature and concentration gradients are relatively small and, as a consequence, the physico-chemical properties are practically uniform throughout the region of interest. The mathematical models are so developed by adopting a given flow field and by considering the local heat and mass balance equations.

For the first model the velocity profile is given by equation (1). As this flow field can be regarded as the fully developed radial flow, this model will be denoted as the "Graetz" type model, in analogy with the work by Graetz for a cylindrical tube [6]. For the other model a linear velocity profile is assumed in the transverse z -direction according to the equation:

$$v_r(r,z) = 6v_m(r) \frac{z}{b}, \quad (3)$$

which accounts for consistency with the parabolic profile in equation (1) in the limit of vanishing values of z . This simplification is justified by the observation, made by L ev eque [7], that, as long as the boundary layers, where the heat and mass gradients are actually constrained, are relatively thin, the relevant velocity profile can be considered nearly linear with the distance from the solid wall. This simple model will be therefore denoted as the "L ev eque" type model. The previous simplification together with that of neglecting the diffusive transport in the r -direction allows one to solve very easily the balance equations with the relevant boundary conditions. Furthermore an explicit expression is obtained for the Sherwood or Nusselt numbers where the influence of the relevant dimensionless groups (Re , Sc or Pr and geometric length ratios) is neatly apparent.

On the other side the "Graetz" type model is much more complex to solve although it can furnish solutions which can be considered the "exact" ones of the problem.

MATHEMATICAL MODELS

In this section the governing equations of the models are described in detail. In both models the velocity fields evaluated in the absence of mass and heat transfer are supposed to hold also during the separation process. Then the balance equations are solved to get temperature and concentration profiles and the heat and mass transfer coefficients.

In view of the very small temperature and composition changes within the liquid bulk, constant fluid properties are taken. In addition the velocity com-

ponent in the z -direction is neglected, assuming pure diffusion for heat and mass transfer in that direction.

L ev eque type model

The L ev eque type model is a simplified approach in which virtually only the boundary layer on the membrane surface is considered to establish the heat and mass transfer coefficients. In such a scheme the velocity field is expressed by the L ev eque approximation, given by equation (3).

As the order of magnitude analysis suggests, the diffusive term in the r -direction can be neglected and the mass balance can be written as:

$$v_r \frac{\partial c_i}{\partial r} + v_z \frac{\partial c_i}{\partial z} = \mathcal{D}_i \frac{\partial^2 c_i}{\partial z^2} \quad (4)$$

with the boundary conditions:

$$c_i = c_{iw} \quad \text{for } z = 0$$

$$c_i = c_{i\infty} \quad \text{for } z \rightarrow \infty,$$

where c_i is the molar concentration of the component i and \mathcal{D}_i is the diffusivity.

It must be pointed out that the clearance b between the disks is finite whereas the second boundary condition is given for $z \rightarrow \infty$. Nevertheless, this boundary condition may satisfactorily represent the physical behaviour as long as the boundary-layer thickness, δ_M , remains significantly smaller than b . The validity of this assumption in the L ev eque model must be therefore checked *a posteriori* and in any case may represent a limit of this model.

Equation (4) combined with equations (2) and (3) gives:

$$A \frac{z}{r} \frac{\partial c_i}{\partial r} = \mathcal{D}_i \frac{\partial^2 c_i}{\partial z^2}, \quad (5)$$

where

$$A = \frac{3\dot{V}}{\pi b^2}.$$

Equation (5) may be transformed into an ordinary differential equation by introducing the following dimensionless quantities:

$$c_i^* = \frac{c_i - c_{iw}}{c_{i\infty} - c_{iw}} \quad \eta = \sqrt{\frac{A}{18\mathcal{D}_i r^2}} z.$$

Then equation (5) becomes:

$$\frac{d^2 c_i^*}{d\eta^2} + 12\eta^2 \frac{dc_i^*}{d\eta} = 0, \quad (6)$$

with the boundary conditions:

$$c_i^* = 0 \quad \text{for } \eta = 0$$

$$c_i^* = 1 \quad \text{for } \eta \rightarrow \infty.$$

Equation (6) can be easily solved and after introducing the relevant boundary conditions the solution is:

$$c_i^* = \frac{\int_0^\eta \exp[-4\eta'^3] d\eta'}{\int_0^\infty \exp[-4\eta'^3] d\eta'} = 1.7776 \int_0^\eta \exp[-4\eta'^3] d\eta' \quad (7)$$

The integrals in equation (7) can be evaluated numerically or through a use of a series [8]. Due to the analogy between heat and mass transfer problems, the same expression holds for the temperature:

$$T^* = 1.7776 \int_0^\eta \exp[-4\eta'^3] d\eta', \quad (8)$$

where:

$$T^* = \frac{T - T_w}{T_\infty - T_w} \quad \eta = \sqrt[3]{\frac{A}{18\alpha r^2}} z \quad \text{and} \quad \alpha = \frac{k}{\rho c_p}$$

From the knowledge of the concentration and temperature profiles, one can easily obtain the values of the mass and heat transfer coefficients, that is the values of the average Sherwood and Nusselt numbers:

$$Sh_{av} = \frac{k_L R}{\mathcal{D}} = 1.849 \left[1 - \left(\frac{R_0}{R} \right)^{4/3} \right] \left(\frac{R}{b} \right)^{1/3} Sc^{1/3} Re^{1/3}, \quad (9)$$

$$Nu_{av} = \frac{hR}{k} = 1.849 \left[1 - \left(\frac{R_0}{R} \right)^{4/3} \right] \left(\frac{R}{b} \right)^{1/3} Pr^{1/3} Re^{1/3}, \quad (10)$$

where:

$$Sc = \frac{\nu}{\mathcal{D}} \quad Pr = \frac{\nu}{\alpha} \quad \text{and} \quad Re = \frac{v_m(r)r}{\nu}$$

in which $v_m(r)$ is the average velocity of the fluid at a given value of the radius r . The transport coefficients appearing in equations (9) and (10) are defined through the empirical relationship for the heat and molar fluxes, respectively, where the driving forces are supposed to be the difference of the temperature and the concentration values between the inlet and the wall at $z = 0$.

Note that, from the definition of Re and the dependence of $v_m(r)$ on r , Re is independent of r . As it is expected, the Nusselt (Sherwood) number does not depend on the values of the temperature (concentration) at the solid wall at $z = 0$, while the parameters entering the problems are the geometric length ratios R_0/R and R/b , and the dimensionless groups Re and Pr (Sc). Anyway the parameter R_0/R can be disregarded as long as it remains substantially smaller than unity.

It must also be observed that, as boundary condition at $z = 0$, a fixed value is assumed for the temperature or concentration. Actually, for the membrane separation processes, this value is not known nor fixed, but the real condition should be somehow

intermediate between that of fixed value and that of fixed flux. In practice, however, this makes a very small difference if the energy or mass flow rate across the membrane is small with respect to that entering the system, as it happens in the existing processes.

Graetz type model

As previously discussed, the solution reported in ref. [1] of the continuity equation:

$$\frac{1}{r} \frac{\partial(rv_r)}{\partial r} + \frac{\partial v_z}{\partial z} = 0, \quad (11)$$

has been used for the Graetz type model to describe the fully developed velocity field between the parallel disks. So a parabolic profile in z -direction results for $v_z(z, r)$ at any given r , as equation (1) reflects.

For the radial geometry the mass and energy balances can be written in cylindrical coordinates as:

$$\frac{1}{r} \frac{\partial}{\partial r} (rv_r \phi) + \frac{\partial}{\partial z} (v_z \phi) = \frac{1}{r} \frac{\partial}{\partial r} \left(r \Gamma \frac{\partial \phi}{\partial r} \right) + \frac{\partial}{\partial z} \left(\Gamma \frac{\partial \phi}{\partial z} \right). \quad (12)$$

In equation (12) for the heat (mass) transfer problem ϕ represents the temperature (mass fraction of the permeating component) and Γ the heat (mass) diffusivity. Referring to Fig. 1 the relevant boundary conditions are:

$$\begin{aligned} \phi &= \phi_0 & \text{for } r = R_0 & \text{ and } 0 \leq z \leq b \\ \frac{\partial \phi}{\partial r} &= 0 & \text{for } r \rightarrow \infty & \text{ and } 0 \leq z \leq b \\ \phi &= \phi_w & \text{for } R_0 \leq r \leq R & \text{ and } z = 0 \\ \frac{\partial \phi}{\partial z} &= 0 & \text{for } R < r & \text{ and } z = 0 \\ \frac{\partial \phi}{\partial z} &= 0 & \text{for } R_0 < r & \text{ and } z = b. \end{aligned} \quad (13)$$

These boundary conditions imply that: (1) the surface at $z = 0$ and for $R_0 \leq r \leq R$ is maintained at a given temperature or concentration as discussed for the Lévêque model; (2) the wall at $z = b$ is everywhere thermally insulated and impermeable; and (3) at high values of the radius no radial variation of the dependent variable takes place as the heat and mass fluxes through the surfaces are constrained at radius smaller than R . In any case different downstream boundary conditions can affect the solution in the region of interest only at a small extent because in the r -direction the convective transport is usually more important than the backstream diffusion. Their relative importance depends of course on the heat or mass Péclet number whose value determines also the extension of the zone of influence of the downstream boundary conditions.

It is easy to realise that, by introducing the same dimensionless quantities of the Lévêque problem, one obtains dimensionless equations where the same dimensionless parameters of the Lévêque problem appear.

The set of the governing equations can be solved by the analytical method outlined by Stevenson [3] and Cooney *et al.* [4]. However, in our opinion a numerical method can be more effectively used for the solution due to the drawbacks suffered by the analytical method which have been analysed in the introduction.

So a finite difference numerical method with a control-volume approach and staggered grids for ϕ and the velocity components has been adopted to discretize and integrate equation (12) with the boundary conditions given by equation (13).

Once one has obtained the ϕ profiles, the fluxes can be calculated across the control volume surfaces and the transfer coefficients can be obtained between the liquid bulk and the solid wall at $z = 0$.

In Fig. 2, the temperature and concentration profiles are reported together with the thickness of the relevant boundary layers vs the radius r . One observes that, due to the smaller value of the mass diffusivity with respect to the heat diffusivity, the mass boundary layer is thinner than the heat boundary layer at every r . Indeed the values of the ratio of the heat boundary layer to that of the mass, reported in Fig. 3 as a function of r/R , remains always larger than unity. It is worth noticing that for the present geometry this ratio is practically independent of Re and is approximately equal to $(Sc/Pr)^{1/3}$, whereas for two parallel plates the order of magnitude estimate would indicate a proportionality to $(Sc/Pr)^{1/2}$.

From Fig. 2 it is apparent that, at low value of Re and at high value of r , it may happen that all the space between the disks is occupied by a temperature gradient. Only at very extreme values of Re and r may the same phenomenon take place for the concentration.

As the L ev eque model leads to an analytical expression for the Nusselt (Sherwood) number as a function of Re , Pr (Sc) and of the ratio R/b , the

influence of these dimensionless parameters can be straightly appreciated from the direct observation of the equations (9) and (10). It is so interesting to investigate if the same influence holds also for the more complete Graetz model. To this aim the results from the Graetz model have been reported in Fig. 4 for one dimensionless number at a time. The expectations, derived from equations (9) and (10) of the L ev eque model, are verified also for the Graetz model. In fact from Fig. 4 the slope of the curves in the log-log plot is approximately 1/3 in most the domain for all the intervening parameters, as equations (9) and (10) suggest. The regions where the slope is no longer 1/3 identify the limits of the L ev eque model. For example, as the Reynolds number decreases, the boundary-layer thickness increases and ultimately becomes as large as the gap between the two disks, so that under these conditions the physical behavior cannot be described any longer by the boundary-layer approximation.

ELABORATION OF EXPERIMENTAL DATA

Measures were taken during vacuum membrane distillation experiments of dilute aqueous mixtures containing ethyl alcohol and some other volatile organic compounds. The experimental set up and the relevant techniques are described in detail in refs. [9, 10].

The apparatus employed is quite similar to a pervaporation experimental set up. The experiments were performed with two different cells, geometrically not similar due to the different values of the ratio between the external radius of the cell, R , and the clearance between the disks, b . In both cases the inlet liquid solution was fed at the center of the cell perpendicularly to the membrane and flowed in radial

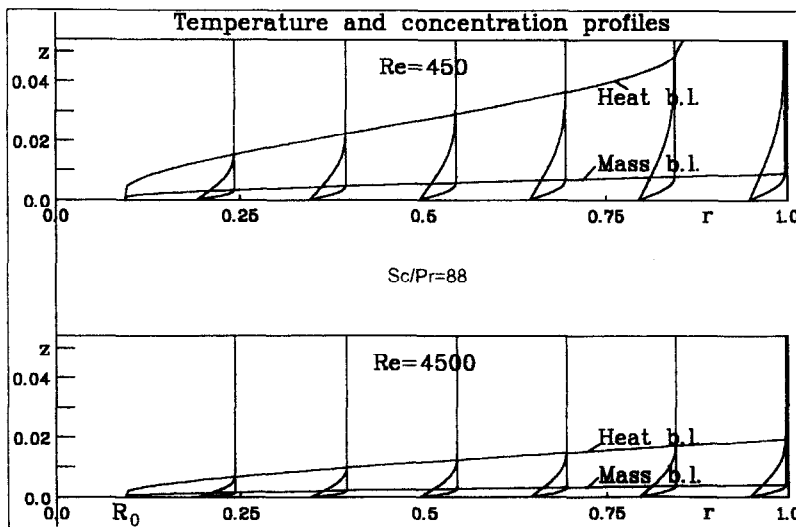


FIG. 2. Temperature and concentration profiles and heat and mass boundary layers for the cell with $R/b = 18.5$ at two different values of the Reynolds number.

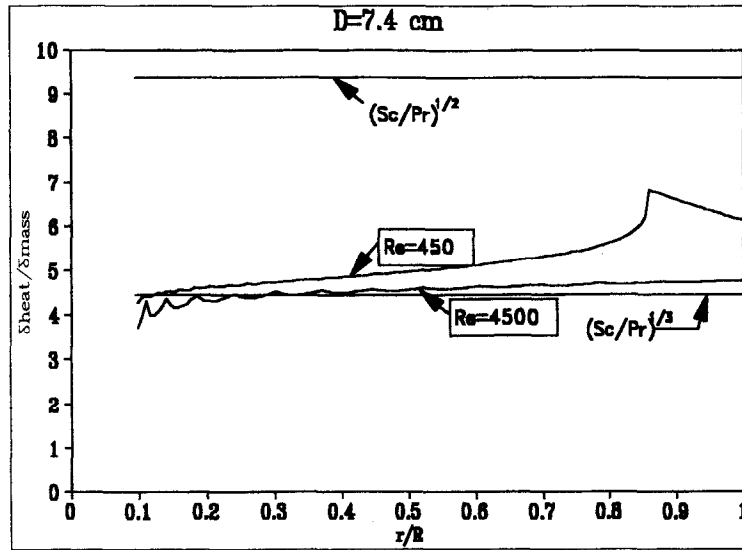


FIG. 3. Ratio between the heat and mass boundary layer thicknesses as a function of the cell radius for $Sc/Pr = 88$ at $Re = 450$ and 4500 .

direction between two parallel disks. A scheme of the apparatus and of the process is given in Fig. 5.

The experimental apparatus enables a direct measurement of the flow rate, the composition and the temperature of the feed, the flow rate, the composition and the pressure of the permeate, the composition and the temperature of the retentate. To calculate the transport coefficients from the experimental data, the local mathematical model of VMD processes was used [9]. In this model the mass transfer coefficient through the liquid phase is calculated according to the film theory model which gives the following relationship [11]:

$$\frac{J_i}{k_L c_L} = \ln \left(\frac{x_{i,I} - J_i/J_i}{x_{i,B} - J_i/J_i} \right), \quad (14)$$

where $x_{i,B}$ and $x_{i,I}$ are the molar fraction of i in the liquid bulk and at the interface, respectively, c_L is the total molar concentration in the liquid phase, J_i and J_i are the molar fluxes.

Inside the membrane the molecular mean free path of the vapor is larger than the pore size (nominal pore

size = 0.01–0.1 μm), so that Knudsen diffusion is the dominant transport mechanism. It follows that the molar flux J_i is linearly related to the partial pressure difference across the membrane [12]:

$$J_i = \frac{K_m}{\sqrt{M_i}} (P_1 y_{i,L} - P_P y_{i,P}), \quad (15)$$

where K_m is the pore permeability and is measured independently by air permeation experiments under the same operating conditions (same average pressure and pressure drop across the membrane).

The total molar flux, J_t , is obtained by taking the sum over all the components:

$$J_t = \frac{K_m}{\sqrt{M}} (P_1 - P_P), \quad (16)$$

in which M is an average molecular weight defined as:

$$\sqrt{M} = \sum_i \frac{J_i}{J_t} \sqrt{M_i}. \quad (17)$$

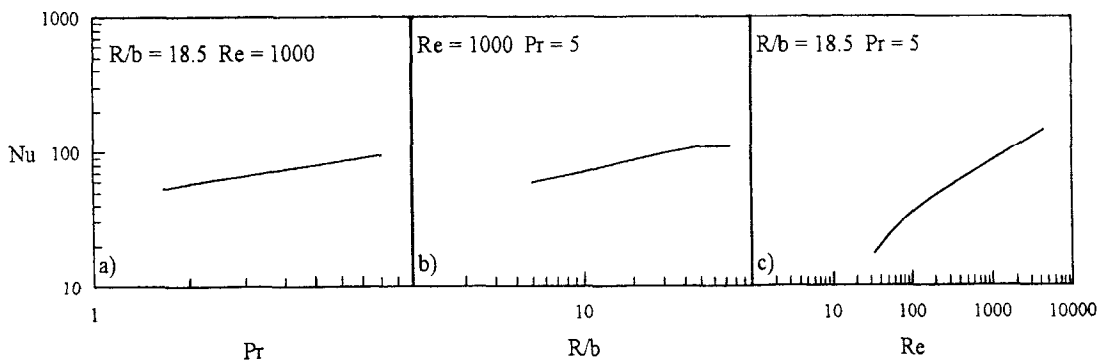


FIG. 4. Nusselt number as a function of different dimensionless groups.

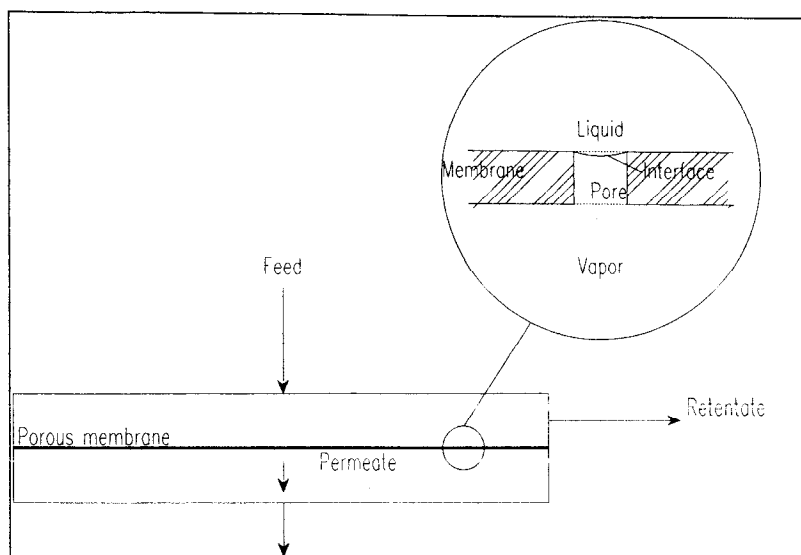


FIG. 5. Scheme of the vacuum membrane distillation (VMD) process.

The heat needed for the evaporation is provided by the liquid feed, and as a consequence the heat transfer coefficient, h , can be calculated from a simple heat balance:

$$\sum_i J_i \tilde{\lambda}_i = h(T_B - T_1), \quad (18)$$

where $\tilde{\lambda}_i$ is the molar latent heat of vaporization for the component i .

The calculation of the transport coefficients requires the knowledge of the vapor-liquid equilibrium at the interface:

$$P_I y_{i,I} = P_i^*(T_I) x_{i,I} \gamma_i, \quad (19)$$

where the activity coefficient, γ_i , can be obtained by using a suitable model for the non-ideal mixture (e.g. Van Laar, Wilson, NRTL).

With the model described above we calculated the heat and mass transfer coefficients for the available experimental data which are reported in refs. [9, 10].

RESULTS

To test the transport models described above the experimental data for the VMD process, reported in refs. [9, 10], have been compared with the model predictions.

Firstly the Sherwood and the Nusselt numbers predicted at different operating conditions by the models are compared with the corresponding measured values for the VMD of various organic-water mixtures in a cell with $D = 7.4$ cm. The results are shown in Fig. 6 for the mass transfer in terms of the Sherwood number and in Fig. 7 for the heat transfer in terms of the Nusselt number vs the Reynolds number.

The agreement is very satisfactory for the mass transfer, whereas for the heat transfer the scatter in the data is a little more noticeable. In any case it can

be concluded that the models can interpret quite well the behavior of the different kind of mixtures investigated. It is worth noting that the predictions by the simpler Lévêque model are as good as the ones by the

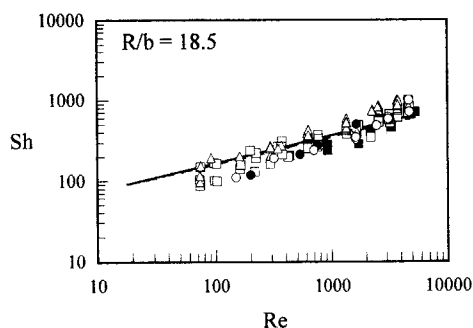


FIG. 6. Comparison between the average Sherwood number predicted by the models of Graetz (—) or Lévêque (---) for VMD of ethyl alcohol (■), isopropyl alcohol (□), acetone (△), methyl acetate (●), ethyl acetate (○) aqueous mixtures.

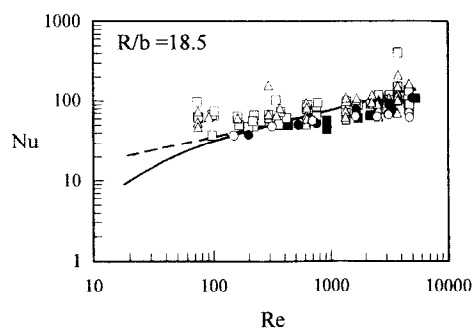


FIG. 7. Comparison between the average Nusselt number predicted by the models of Graetz (—) or Lévêque (---) for VMD of ethyl alcohol (■), isopropyl alcohol (□), acetone (△), methyl acetate (●), ethyl acetate (○) aqueous mixtures.

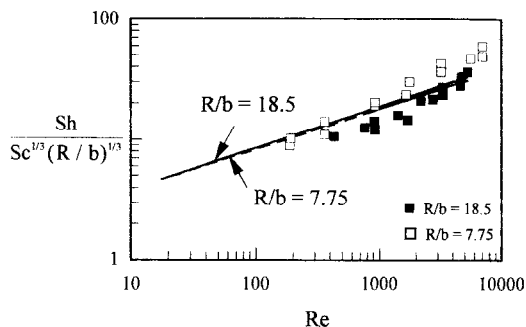


FIG. 8. Comparison of the predictions by the Graetz model and the experimental data for VMD of ethyl alcohol aqueous mixtures for two cells of different diameter: dimensionless group $Sh/[Sc^{1/3}(R/b)^{1/3}]$ as a function of Reynolds number.

Graetz model, since deviations between the results by the two different models take place only in regions of minor practical interest.

It must be also pointed out that the models have no adjustable parameters, as all the intervening flow and physico-chemical properties have been measured or evaluated independently.

For ethyl alcohol–water mixtures the data available for two cells, with different diameters, but with the same clearance, were compared with the predictions of the Graetz model to investigate the influence of the geometric ratio R/b . Indeed the two cells are not geometrically similar due to the difference in the ratio R/b . In this case it is advisable to plot the results in terms of the ratio $Sh/[Sc^{1/3}(R/b)^{1/3}]$, or $Nu/[Pr^{1/3}(R/b)^{1/3}]$ vs the Reynolds number (see Figs. 8 and 9). The agreement is still satisfactory. In the case of heat transfer the model predictions for the two cells deviate significantly from each other at low Reynolds numbers. Indeed at these fluid dynamic regimes the heat boundary layer may occupy the whole space between the disks for the larger radii pertaining to the $D = 7.4$ cm cell, whereas the same phenomenon does not take place in the smaller cell. Such a behavior is not observed in the case of mass transfer in the range of Reynolds numbers of practical

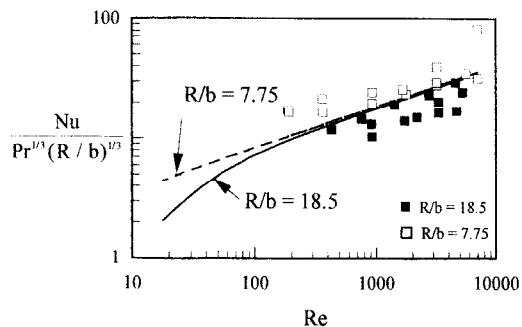


FIG. 9. Comparison of the predictions by the Graetz model and the experimental data for VMD of ethyl alcohol aqueous mixtures for two cells of different diameter: dimensionless group $Nu/[Pr^{1/3}(R/b)^{1/3}]$ as a function of Reynolds number.

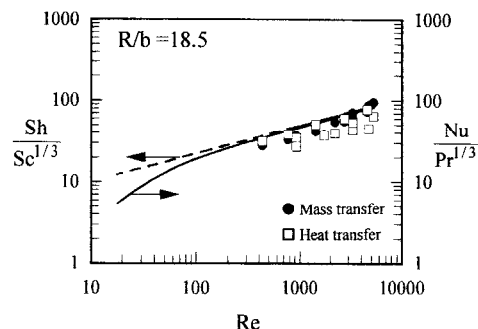


FIG. 10. Comparison of the predictions by the Graetz model and the experimental data for VMD of ethyl alcohol aqueous mixtures: dimensionless groups $Sh/Sc^{1/3}$ and $Nu/Pr^{1/3}$ as a function of Reynolds number.

interest here investigated, as it is apparent in Fig. 10 where the ratios $Sh/Sc^{1/3}$ and $Nu/Pr^{1/3}$ are plotted vs the Reynolds number. This is a consequence of the fact that the mass boundary layer remains thinner than the clearance between the disks, as already discussed.

CONCLUSIONS

An analysis of the heat and mass transfer in radial flow between two parallel disks has been performed with the use of two different mathematical models. The results obtained with the examined models have been compared with the experimental data available for the VMD process. In general the adopted models even with no adjustable parameters do reproduce with good accuracy the behavior of the system in the range of practical interest.

The results from the simple L ev eque model agree very well with the ones from the more complex Graetz model, so that the simpler model can be effectively used in most of the cases. They deviate significantly only in the case of heat transport at very low Reynolds numbers, where the heat boundary layer may extend over the whole space between the parallel disks. As usual, the mass boundary layer is always thinner than the heat boundary layer and the ratio of the heat to the mass boundary-layer thickness depends on the physical properties, but with a dependency which is different from that experienced in other geometries.

For both the models, the transport coefficients depend on the physical properties, the geometry of the system and the flow rate. The relevant relationships among the dimensionless parameters entering the problem have been identified and they reflect the singular behavior that pertains to the radial flow.

Acknowledgement—The authors wish to thank Dr Serena Bandini for her helpful contribution to the discussion of the experimental results.

REFERENCES

1. R. B. Bird, W. E. Stewart and E. N. Lightfoot, *Transport Phenomena*, p. 114. John Wiley, New York (1960).

2. H. Schlichting, *Boundary-Layer Theory*, p. 87. McGraw-Hill, New York (1968).
3. J. F. Stevenson, Heat and mass transfer in radial flow, *Chem. Engng Sci.* **31**, 1225–1226 (1976).
4. D. O. Cooney, S.-S. Kim and E. J. Davis, Analyses of mass transfer in hemodialyzers for laminar blood flow and homogeneous dialysate, *Chem. Engng Sci.* **29**, 1731–1738 (1974).
5. R. M. Ybarra and R. E. Eckert, Transport eigenvalue problems—effect of order of approximation and step size on solution accuracy, *A.I.Ch.E. Jl* **31**, 1755–1757 (1985).
6. L. Graetz, Über die wärmeleitfähigkeit von flüssigkeiten, *Ann. Phys. Chem.* **25**, 337–357 (1885).
7. J. Lévêque, Les lois de la transmission de chaleur par convection, *Ann. mines* **13**, 201–239 (1928).
8. M. Abramowitz, *J. Math. Phys.* **30**, 162 (1951).
9. G. C. Sarti, C. Gostoli and S. Bandini, Extraction of organic components from aqueous streams by vacuum membrane distillation, *J. Membrane Sci.* **80**, 21–33 (1993).
10. A. Saavedra Fenoglio, Distillazione a membrana sotto vuoto: studio teorico-sperimentale applicato all'estrazione di composti organici volatili da soluzioni acquose, Ph.D. Thesis, University of Bologna, Bologna, Italy (1993).
11. M. C. Porter, Concentration polarization with membrane ultrafiltration, *Ind. Eng. Chem., Prod. Res. Dev.* **11**, 234–248 (1972).
12. S. Bandini, C. Gostoli and G. C. Sarti, Separation efficiency in vacuum membrane distillation, *J. Membrane Sci.* **73**, 217–229 (1992).